Research on Engineering Structures & Materials
www.jresm.org
Research Group

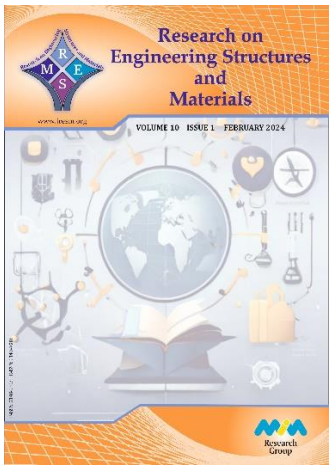

Effects of seawater and acidic environment on mechanical properties of iron powder-loaded glass-epoxy composite laminates: Experimental and analytical investigation

Youcef Gheid, Abdennacer Chemami, Djamel Gaagaia, Hamza Aouaichia

Online Publication Date: 24 January 2024
URL: http://www.jresm.org/archive/resm2024.116me1207rs.html
DOI: http://dx.doi.org/10.17515/resm2024.116me1207rs

To cite this article
Gheid Y, Chemami A, Gaagaia D, Aouaichia H. Effects of seawater and acidic environment on mechanical properties of iron powder-loaded glass-epoxy composite laminates: Experimental and analytical investigation. *Res. Eng. Struct. Mater.*, 2024; 10(3): 1109-1123.

Research on Engineering Structures & Materials
www.jresm.org
Research Group

Research Article

Effects of seawater and acidic environment on mechanical properties of iron powder-loaded glass-epoxy composite laminates: Experimental and analytical investigation

Youcef Gheid*[1,a], Abdennacer Chemami[1,b], Djamel Gaagaia[2,c], Hamza Aouaichia[3,d]

[1]Industrial Mechanics Laboratory, Dept. of Mechanical Eng., Badji Mokhtar-Annaba University, Algeria
[2]Dept. of Mechanical Eng., Badji Mokhtar-Annaba University, Algeria
[3]Research Center in Industrial Technologies CRTI, Algeria

Article Info

Article history:

Received 07 Dec 2023
Accepted 24 Jan 2024

Keywords:

Composite laminate;
Iron powder;
Flexure strength;
Hydrochloric acid;
Seawater;
Immersion

Abstract

This study assesses the impact of seawater and acidity on a glass epoxy composite filled with pure iron powder. Plates with varying iron content (15%, 20%, and 25%) were created using contact molding, with 30% glass fiber content. After dividing the plates into samples, a three-point bending examination was conducted following ISO14125 standards. The samples were immersed in saltwater (Group A), an acidic solution (Group B), or kept dry for comparison (Group C). Each subgroup had 15 specimens (5 for each iron %), immersed for over 60 days before undergoing bending tests. Results showed a significant decline in flexural strength, with a maximum reduction of 29.7% in Group A and 37.9% in Group B, while Young's modulus decreased up to 34.8% in Group A and 45.6% in Group B. The two-way ANOVA approach confirmed these findings, and microscopic examinations and FTIR analysis after immersion elucidated physical alterations and chemical reactions. Despite certain advantages, such as specific applications, the composite's limitations in corrosion resistance, durability, and production cost may restrict its relevance in various industrial and real-world applications. Consideration of these factors is essential before choosing this material for a specific project.

1. Introduction

In recent years, the use of fiber-reinforced composite materials in engineering has grown significantly. This increase is due to advances in how these materials are made, making them more suitable for various technical uses [1]. Industries like aerospace and automotive are particularly interested in lightweight materials that are also strong, leading to a higher demand for composite materials [2].

One specific type of these materials, known as glass-epoxy composites, reinforced with various substances, including different metals, has become important in different industries because of its exceptional strength [3]. Researchers have studied how adding different metals, like iron powder, affects the strength of these materials [4-7].

Previous research has examined the impact of nanoparticles on the micro-mechanical and surface properties of poly (urea-formaldehyde) composite microcapsules [8]. Additionally, they have explored the thermo-mechanical behavior of epoxy composites, incorporating various fillers like E-glass fibers and iron oxide particles, as well as the mechanical

*Corresponding author: youcef.gheid@univ-annaba.dz
[a] orcid.org/0000-0002-8561-6757; [b] orcid.org/0009-0005-5754-6324; [c] orcid.org/0000-0002-4645-2884; [d] orcid.org/0000-0003-0272-5446
DOI: http://dx.doi.org/10.17515/resm2024.116me1207rs

performance of glass/epoxy composites enriched with micro- and nano-sized aluminum particles [9, 10]. Other studies have delved into composite materials that include iron powder and mixed glass fiber-reinforced polymers, with the aim of comprehending their properties and performance. Besides, researchers have examined the use of waste iron filings to enhance glass fiber-reinforced epoxy (GFRE) composites, analyzing the influence of factors such as particle size, interface adhesion, and loading on particulate-polymer composites [11, 12].

Despite their strength, these composites face challenges when they are exposed to harsh conditions. Prolonged exposure to corrosive substances like acids or seawater can significantly weaken these materials, especially in terms of their flexural strength [13]. Epoxy resins are used to hold these materials together and protect them from harsh conditions like water and salt [14]. However, epoxy can absorb moisture over time, which can harm its physical properties and the components made with it [14]. Abdel-Magid et al. studied the effects of seawater and temperature on glass/epoxy and glass/polyurethane composites. After a year of immersion, glass/epoxy composites absorbed 2.5% of their weight in water at ambient temperature and 5% at 65°C. Tensile strength reduced by 0.8% at room temperature and 6% at 65°C, indicating accelerated water absorption and reduced strength at higher temperatures [15]. Silva et al. explored the degradation of GFRP laminates through 2500 hours of immersion in a saline solution. Tensile strength retention was 84% at 35°C, 70% at 50°C, and 61% at 65°C, revealing swelling and plasticization in the GFRP composites, leading to microcracking and fractures [16]. A study explores the enhanced mechanical resilience of SiO2-epoxy polymer nanocomposites in seawater, revealing minimal strength reduction compared to unmodified materials, with optimal performance achieved at a 3% SiO2-epoxy ratio over a six-month exposure period [17]. Other researchers evaluated the impact of corrosive conditions on epoxy nanocomposites with BN nanoplatelets, enhancing mechanical and tribological properties. And found that, despite the corrosive influence on mechanical performance, tribological behavior improves with exposure, acting as a lubricant and forming a protective layer [18].

Researchers have conducted numerous studies on the impact of water and seawater on GFRP composites, assessing factors like flexural strength, tensile strength, compressive strength, and elastic modulus [19, 20]. Bagherpour et al. examined the effects of concentrated HCl on aged fiber glass polyester composites. After 21 days of acid immersion at 35°C, a significant destructive impact was observed, as acid infiltrated the composite, forming cavities and cracks, and reducing mechanical properties [21]. Additionally, the flexure strength and modulus of elasticity in a glass fiber/epoxy composite decreased over time when exposed to hydrochloric acid (HCl) and sodium hydroxide (NaOH), resulting in mechanical degradation [22]. Similar degradation was observed in Kevlar/epoxy and carbon/epoxy laminates subjected to low-velocity impact tests following immersion in HCl and NaOH [23].

While previous research has contributed significantly to our understanding of how glass-epoxy composites behave in challenging conditions, there are still important questions that need to be investigated regarding the behavior of these laminates, specifically when they are loaded with iron powder in such conditions. This study aims to fill these knowledge gaps by examining how the amount of iron powder, along with environmental conditions, affects the flexural strength of glass-epoxy laminated composites. We will use statistical analysis (ANOVA) to evaluate their relative impacts and potential interactions. The inclusion of iron powder is of particular relevance, given its abundance in the Annaba region, situated in the eastern part of Algeria, due to the presence of the sedimentary iron complex. Beyond addressing material availability, this choice aligns with sustainable practices, emphasizing the repurposing of waste materials.

2. Materials and Methods

2.1. Specimen's Preparation

The laminated composite plates were prepared in the laboratory, using epoxy resin as matrix and reinforced with eight (08) plies of an E-glass fiber mat, which was kept constant at 30% of the total mass for each plate. Additionally, pure iron (99.998%) powder with grain sizes equal to or smaller than 32µm was incorporated as a filler material, with varying percentages of the filler (15%, 20%, and 25%). The laminates were produced by hand lay-up technique, with the resin of choice being a commercially available epoxy, selected based on its local market availability. Densities of the matrix and reinforcement are presented in Table 1. The iron powder was combined with resin and hardener and afterward introduced into a controlled environment equipped with a vacuum pump to facilitate the removal of entrapped air bubbles. According to the epoxy manufacturer's instructions, the polymerization process can take up to seven (07) days.

Table 1. Material's densities

Material	Density (g/cm^3)
Mat fiberglass E	2.7
Epoxy resin	1.1

The bending specimens illustrated in Figure 1 were dimensioned in accordance with the standards stated in the ISO 14125 standard. An 1100 W CROWN cutting machine equipped with a 250mm diameter diamond disc and a lubrication system was utilized to cool the specimens and aid in the cutting process.

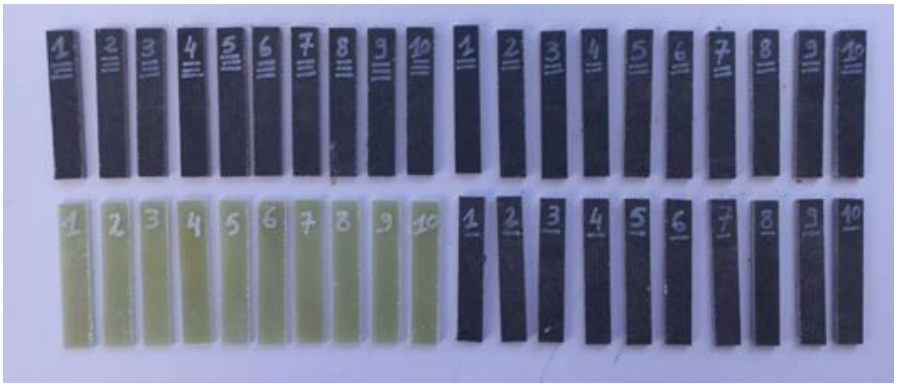

Fig. 1. Laminated specimens

2.2 Solution Preparation

Two discrete forms of media were generated for the purpose of conducting experiments. The initial medium was prepared by utilizing seawater obtained from a coastal area in the Annaba region. Following the collection process, the specimen underwent a rigorous sterilization procedure, subsequently undergoing meticulous drying within specialized ovens. The second medium was prepared as shown in Figure 2 by diluting pure hydrochloric acid (HCl) with distilled water until it reached a pH value of 2. Similar to the initial medium, this subsequent medium likewise underwent a process of sterilization and subsequent drying through the utilization of specialized ovens. These preparations will enable the submersion of the test specimens that have been prepared for our forthcoming tests.

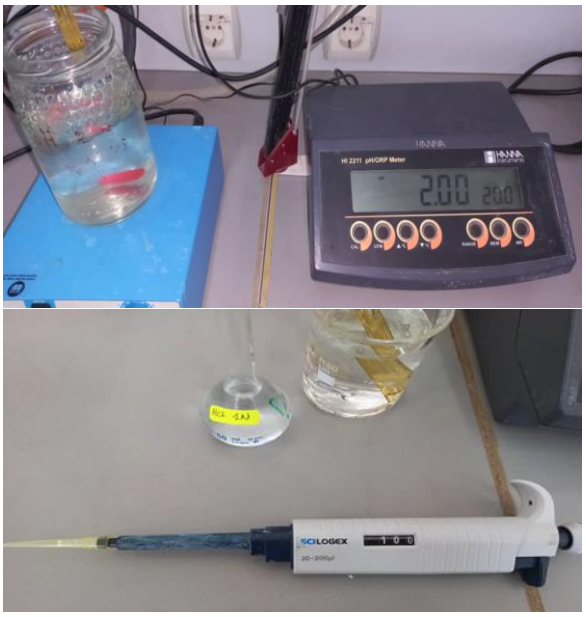

Fig. 2. Acidic solution preparation

3. Experimental Procedure

The specimens were partitioned into three distinct groups as demonstrated in Table 2, denoted Group A, Group B and Group C. Within Group A, three subgroups were exposed to seawater, whilst the three B subgroups were submitted to an acidic solution with a pH value of 2, while the remaining subgroups stay unsubmerged for comparison.

Table 2. Specimen's grouping

Group	Subgroups	Iron content (W%)	Solution
A	A-1	15	Seawater
	A-2	20	Seawater
	A-3	25	Seawater
B	B-1	15	Acid
	B-2	20	Acid
	B-3	25	Acid
C	C-1	15	/
	C-2	20	/
	C-3	25	/

3.1 Submersion's Impact on Specimen Weight

The dry non immerged, and immerged specimens were weighed to measure W_o, submerged in the two different solutions for no less than 1440 hours, where the samples were removed to measure their individual weight as shown in Fig. 3, W_i, for each time interval, using an analytical balance with a resolution of 0.0001g resolution. The weight measurements are detailed in table 3, in which:

- T0 (Time Zero): Refers to the initial time when the specimens are submerged or subjected to the experimental conditions.
- T1 to T6: These time points represent specific intervals during the experiment, indicating when measurements or observations were taken. For instance, T1 might signify measurements taken after 10 days, T2 after 20 days, and so forth. Each subsequent time point (T3, T4, T5, and T6) would similarly denote additional intervals or milestones in the experiment, helping to track changes over time.

Fig. 3. Weight measurement operation

Table 3. Specimen's weight measurement detailed

Group	Sub-group	T0	T1	T2	T3	T4	T5	T6
A	1	7.6049	7.6070	7.6085	7.6098	7.6123	7.6246	7.6655
	2	7.957	7.9608	7.9620	7.9636	7.9649	7.9755	7.9989
	3	8.4760	8.4807	8.4835	8.4837	8.4865	8.4964	8.5227
B	4	7.5305	7.5275	7.5244	7.5253	7.5175	7.513933	7.5152
	5	7.8348	7.8326	7.8303	7.8301	7.8231	7.8163	7.8026
	6	8.8055	8.8005	8.7974	8.7889	8.7817	8.7808	8.7616

3.2 Moisture Absorption

Measuring moisture absorption of the studied specimens has been done using the simple formula in Eq. (1) as follows:

$$\% = (W_i - W_0) \div W_0 \quad (1)$$

Where, W_0 is the initial weight of samples, W_i is the weight of samples after up taking moisture.

3.3 Flexure testing

The 3-points flexure testing schematized in fig. 4, was conducted at the "Mining and Metallurgy Research Unit", formerly known as "URMA", which is a part of the "Research Centre in Industrial Technologies" (URMM/CRTI) located in Annaba (Algeria). The MTS 43, a universal machine, is outfitted with a force sensor and is under the control of a computer. A minimum of five (5) tests were applied for each subgroup, using specimens mean dimensions displayed in Table 4. In this case, speed and temperature were 10 mm/min and 25 °C, respectively. The load cell illustrated in Fig. 5, also known as a dynamometer, is

linked to an acquisition chain that enables the concurrent measurement of displacement time, load, and deformation. The data collection and result processing were conducted using computer technology, specifically the MTS TestSuite software. A total of 6 experiments and combinations of variables were conducted, in order to measure the flexural strength and Young's modulus.

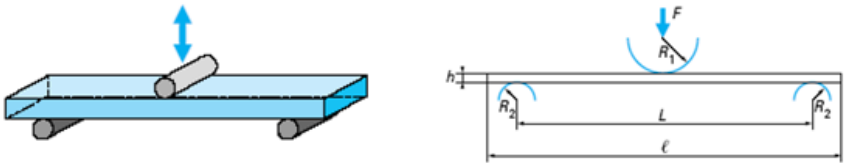

Fig. 4. Three points bending scheme

Table 4. Specimen mean dimensions

Length (l) mm	Outer span (L) mm	Width (b) mm	Thickness (h) mm
80	64	14	4

(a) (b)

Fig. 5. Bending test procedure (a) and (b)

3.4 Microscopic and FTIR Equipment

Observations of microfibrils, surface topography, and the rupture area were conducted using a light microscope. The type of microscope equipment used for this research was the Leica ATC 2000 Microscope, Wetzlar.

Meanwhile, the FTIR spectra were recorded at the “Water and Environmental Science and Technology Laboratory” located in University Mohamed Cherif Messaidia, Souk Ahras, Algeria, using an IRAffinity-1S FTIR at a measuring range between 500 and 4000 cm^{-1}

4. Results and Discussion

4.1. Submersion’s Impact on Specimen Weight

This study employed a Two-Way ANOVA approach to examine the variations in the weight of the specimens when subjected to immersion in two distinct solutions for ne less than 60 days: a seawater environment and an acidic solution. The present investigation took into account the variables of immersion duration and the proportion of iron powder loading.

The outcomes exhibited noteworthy disparities in comparison to the specimens that were not subjected to immersion, which can be referred to as the control group (C).

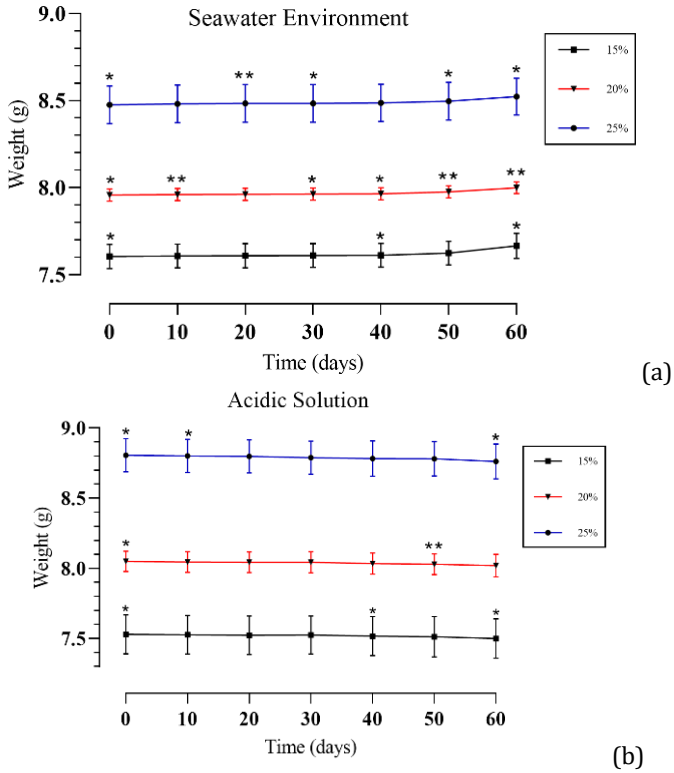

Fig. 6. Charts (a) and (b) display the evaluation of the masses of various test specimens over time

Compared with the control, the weight change illustrated in Fig. 6 was significant ($p < 0.05$), proportional to the time of immersion. In such a way a noticeable increase in weight was observed over time in specimens immersed in seawater (Fig. 6-a), indicating significant water absorption. This aligns with findings from Abdel-Magid et al., who reported increased water absorption in glass/epoxy composites exposed to seawater over a year, supporting the impact of seawater on weight gain in composite materials [15]. On the other hand, specimens that were fully submerged in the acidic solution exhibited a weight reduction (Fig. 6-b) that was directly related to the duration of exposure. This echoes the findings of Bagherpour et al., who investigated the effects of concentrated HCl on aged fiber glass polyester composites [21]. This weight decrease phenomenon could be attributed to corrosion and material degradation. In corrosive environments like acidic solutions, the chemical reactions involving the iron powder within the composite may release iron ions, leading to material corrosion. This corrosion process contributes to the observed loss of material mass, aligning with Bagherpour et al.'s observations of significant destructive impacts in acid-immersed composites.

4.2 Moisture absorption and Weight loss

The process of moisture absorption was quantified for specimens that were submerged in seawater (Table 5). It was shown that these specimens exhibited moisture absorption, leading to a subsequent increase in their overall weight. On the other hand, the specimens

that were submerged in the acidic solution exhibited a reduction in mass as shown in Table 6.

Table 5. Sub-groups moisture absorption

Sub-group	Absorption (%)
1	0.79
2	0.52
3	0.55

Table 6. Sub-groups weight loss

Sub-group	Weight loss (%)
1	0.20
2	0.41
3	0.50

A direct correlation is noted between the quantity of iron powder present in the laminate and the corresponding reduction in moisture absorption. Stated otherwise, an increase in resin content corresponds to an increase in the moisture absorption capacity of the composite material. Furthermore, it was observed that the test specimens, when subjected to immersion in the acidic solution, exhibited a reduction in weight that was directly proportionate to the quantity of iron contained within them. The observed reduction in weight can be ascribed to the deterioration of the composite material caused by the influence of hydrochloric acid (HCl), as mentioned before.

4.3. Flexure Strength and Young Modulus

4.3.1 Experimental Result Detailed

The analysis focused on the results obtained from a three-point bending experiment carried out on specimens that underwent immersion for a minimum period of 60 days. Figure 7 illustrates the typical stress/strain curve for each group, with detailed results of Flexural Strength and Young's Modulus for each subgroup presented in Table 7.

In such a case that, Fig. 7(a) depicts the stress/strain plot for the subgroup submerged in seawater. In Fig.7(b), the stress/strain plot illustrates the performance of the subgroup submerged in an acidic solution. Finally, Fig. 7(c) presents the stress/strain plot for the non-submerged subgroup, referred to as the control group.

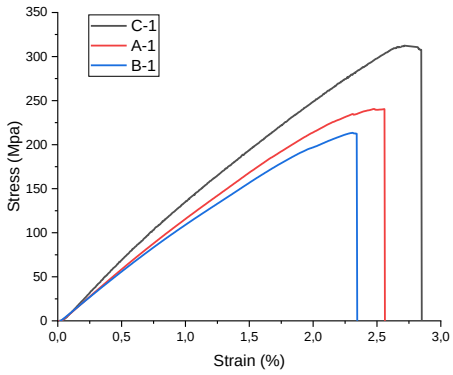

(a)

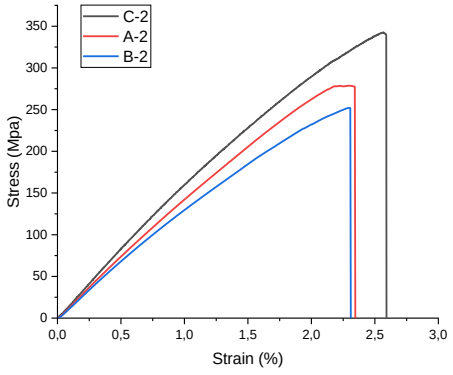

(b)

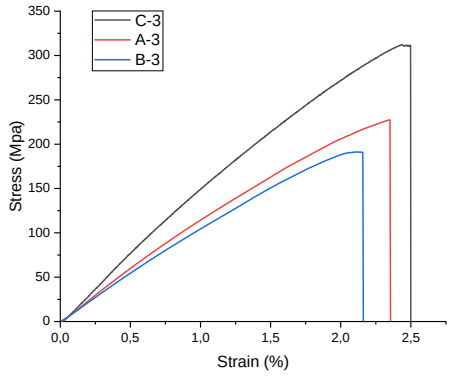

(c)

Fig. 7. Typical plot of Flexure Stress (Mpa) against strain (%)

Table 7. Three points bending test results detailed

Group	Subgroups	Iron content (W%)	Solution	Flexure Strength (Mpa)	Young's Modulus (Mpa)
A	1	15	Seawater	240.5714	10211.82
	2	20	Seawater	263.7119	11162.67
	3	25	Seawater	219.1429	9830.429
B	1	15	Acid	201.5714	8961.479
	2	20	Acid	243.9256	9588.857
	3	25	Acid	193.5714	8200.84
C	1	15	/	310.822	15107.267
	2	20	/	341.198	16366.777
	3	25	/	311.998	15097.248

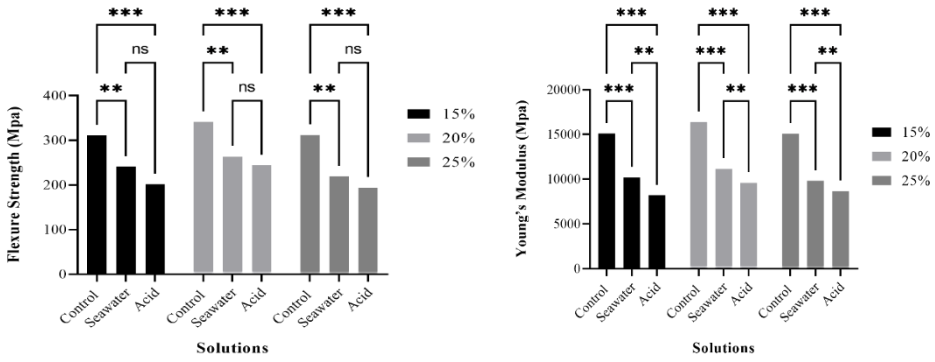

(a) (b)

Fig. 8. ANOVA study charts for Flexural Strength (a) and Young's modulus (b).

The present investigation utilized a Two-Way ANOVA approach to investigate the changes in flexure strength and Young's modulus. The current study considered the factors of flexural strength and Young's modulus, as well as the solution type and iron powder loading %. The results (as shown in Fig. 8) displayed significant differences when

compared to the samples that were not exposed to immersion, which can be referred to as the control group (C). The observed reduction in both flexure strength and Young's modulus was found to be statistically significant when compared to the control group ($p < 0.05$).After the results were evaluated using the ANOVA method, the findings of the study (Fig. 8) demonstrated a significant decrease in both flexural strength and Young's modulus in the immersed composites as compared to the composites that were not subjected to immersion.

The Flexure Strength of Composites 1, 2, and 3 (Fig. 8-a) in Group A decreased by 22.6%, 22.7%, and 29.7%, respectively. Likewise, within group B, laminates 1, 2, and 3 demonstrated a reduction in their flexural strength of 35.1%, 28.5%, and 37.9% correspondingly.

When examining Young's modulus (Fig. 8-b), it was observed that Group A, immersed in seawater, experienced reductions of 32.4%, 31.8%, and 34.8% in subgroups 1, 2, and 3, respectively, when compared to their non-immersed counterparts. In contrast, Group B, exposed to the acidic solution, demonstrated a more substantial decline, with decreases of 40.6%, 41.4%, and 45.6% in subgroups 1, 2, and 3, respectively, compared to their non-immersed counterparts. These findings underscore the significant impact of the acidic solution on Young's modulus in comparison to the specimens not subjected to immersion.

A notable observation was made while comparing the specimens that underwent immersion in an acidic solution with those that were exposed to seawater, as a more prominent reduction in both flexural strength and Young's modulus was observed. In line with the observations from the study conducted by A. M. Amaro et al. [22], the results obtained similarly highlight a notable reduction in flexural strength and Young's modulus for specimens immersed in an acidic solution compared to those exposed to seawater. This correspondence further underscores the higher reactivity of acidic solutions and the consequent mechanical degradation observed in laminates, as indicated in the mentioned study.

The results presented above emphasize the need to consider environmental factors when evaluating the durability and effectiveness of composite materials in real-world situations.

4.4 Microscopic and FTIR analysis

The microscopic photos depict the specimen's immersion in an acidic solution, both before and after the immersion process. These images demonstrate the formation of pores on the epoxy layer (Fig. 9-a-b), which functions as the matrix for the specimen. The observed phenomena elucidate the notable decline in the mechanical strength of the specimens when subjected to immersion in the acidic solution.

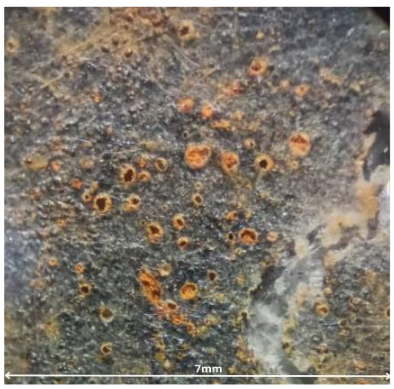

(a)

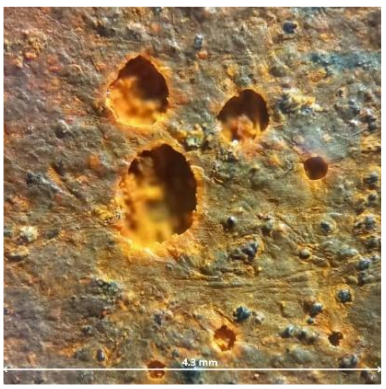

(b)

(c)

Fig. 9. Microscopic images of the surfaces of the specimens immersed in the acid solution (a) (b) and seawater (c)

(a)

(b)

Fig. 10. Microscopic images of the fracture surface of a test specimen (a) (b)

The microscopic images in Fig. 10 reveal the oxidation of iron grains within the glass fibers, which led to a reduction in the mechanical properties of the various specimens. The diagram of the Fig.11 displays the FTIR spectra of distinct specimens while immersed in different solutions: seawater, a pH 2 acid medium, and specimens that were not immersed. The absorption peaks occur at a frequency of 3865 cm^{-1}, which is specifically related to the stretching vibration of hydroxyl (-OH) bonds found in functional groups like water or other hydroxylated compounds. This frequency range also includes values between 3800 and 3900 cm^{-1}. Seawater inherently contains hydroxyl groups.

The frequency at 3734 cm^{-1} corresponds to the stretching vibration of a carbonyl (C=O) bond present in specific organic or inorganic compounds, including corrosion products prevalent in the maritime environment or due to the iron powder presence in our composite.

The peak observed at 1743 cm^{-1} corresponds to the stretching vibration of the C=O bond in the -COO- functional group. Additionally, the peaks at 1473 cm^{-1} and 1373 cm^{-1} are associated with the bending vibration of the -CH3 groups in the -CH (CH3)2 moiety. The peak observed at 1242 cm^{-1} corresponds to the stretching vibration of the C-O bond in the -COOH functional group, while the peak at 1172 cm^{-1} is attributed to the stretching

vibration of a C-O bond. These could be found in functional groups such as esters, ethers, or the vibration of the C-O-C skeleton.

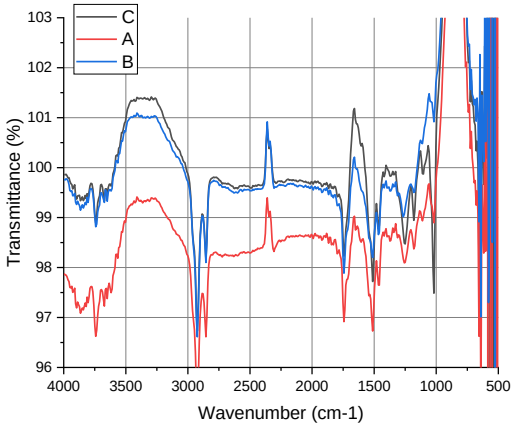

Fig. 11. Diagram of FTIR spectra for different specimens

The predominant peak belongs to the epoxy cycle within the region of 1270-1240 cm^{-1}. The epoxy functions exhibit strong absorption at 1257 cm^{-1}, which corresponds to the symmetrical vibrations of C-O-C. Additionally, there are two peaks at 1153 cm^{-1} that correspond to the vibrations of CH2 groups in the epoxy. The absorption at 3410 and 3382 cm^{-1} in amines is attributed to the vibration of primary amine groups (-NH2) in the hardener structure [24].

The intense peak observed at 2931 cm^{-1} and 2870 cm^{-1} in other groups is associated with the CH groups of the alkane function, and its absorption limit occurs at 1567 cm^{-1}. Ether groups exhibit two distinct absorption peaks at 1257 and 1233 cm^{-1}. The first peak corresponds to C-O-C groups that are connected to aromatic cycles, while the second peak arises from the phatic stretching of carbon-oxygen (-O-CH2) bonds [25].

Epoxy contains functional groups known as epoxy groups (C-O-C) which have the ability to undergo a reaction with water. The three spectra exhibit a high degree of similarity. Nevertheless, alterations in the absorption bands linked to these functional groups, particularly in the range of 1018 to 1735 cm^{-1}, may suggest chemical modifications associated with water absorption. This is evident in the changes observed in the bands at 1018 cm^{-1}, 1118 cm^{-1}, the 1249 cm^{-1} vibration band, and the 1365 cm^{-1} band, which affect the bonding bands.

Water absorption can cause the polymeric matrix to become softer, and acid can affect iron powder, leading to alterations in bonding vibration bands. The absorption bands related to C-C and C-O-C groups in the epoxy matrix may exhibit alterations that indicate modifications in the polymeric structure, as evidenced by the images showing cavities in the material matrix.

The absorption peak observed at 1404 cm^{-1} corresponds to the presence of carbon-nitrogen bonds (CN). Additionally, the range between 1172 and 1200 cm^{-1} is commonly linked to the stretching vibrations of C-N bonds in primary amines. Secondary and tertiary amines can also display bands in this region. However, the position of these bands may vary significantly depending on the characteristics of the group.

The presence of an absorption band at 1249 cm^{-1} in an infrared spectrum can be indicative of many chemical bonds: CO (carbon-oxygen bonds): The stretching vibrations of CO bonds

can be linked to this particular location. It may also exist in functional groups like esters, ethers, or other molecules that have carbon-oxygen linkages. The presence of amines or nitriles can also result in stretching vibrations of CN bonds, which can contribute to this region.

Volenik's research demonstrates that a spectral peak at 1100 cm^{-1}, accompanied by a smaller peak at 1198 cm^{-1}, can be attributed to the vibrational motion of Si-O bonds in SiO2 [26].

5. Conclusions

The immersion of test samples containing varied proportions of iron powder (15%, 20%, 25%) in two distinct solutions (seawater and an acidic solution with a pH of 2) resulted in a notable decrease in mechanical characteristics, particularly in terms of flexural strength and Young's modulus. The drop confirmed using statistical ANOVA analysis, was 40% for specimens submerged in the acidic solution and 30% for those in seawater, highlighting the corrosive properties of the acidic environment. Furthermore, a clear link was observed between the proportions of iron powder loading.

The microscopic images offered a convincing elucidation for the decline in mechanical characteristics, as they unveiled the appearance of pores on the surfaces of specimens submerged in the acidic solution and severe corrosion in those exposed to saltwater. In addition, FTIR analysis provided a clear understanding of the chemical processes that took place in response to the various solutions.

This type of composite, composed of pure iron powder and epoxy fiberglass, has significant limitations for use in industrial or real-world applications. Firstly for its sensitivity to immersion, as the study has shown, immersion in seawater or an acidic solution has a significant impact on the mechanical properties of this composite. The reduction in flexural strength and Young's modulus can make this material unsuitable for applications that require high durability in humid or corrosive environments. Secondly its limited lifespan due to the rapid degradation of mechanical properties under immersion, this composite may have a limited lifespan in applications such as shipbuilding, marine structures, or chemical equipment requiring long-term corrosion resistance.

This composite, while unsuitable for corrosion-sensitive applications, finds relevance in non-corrosive environments, low-stress structural components, and cost-effective projects. Ideal for temporary structures and niche applications, its unique properties cater to demands beyond corrosion resistance. Acknowledging limitations, careful project consideration can unveil tailored applications for this composite, offering a balance of performance and cost-effectiveness. This composite can find application in non-corrosive environments, low-stress structural components, and cost-effective projects. Ideal for temporary structures and niche applications, its unique properties cater to demands beyond corrosion resistance. Acknowledging limitations, careful project consideration can unveil tailored applications for this composite, offering a balance of performance and cost-effectiveness.

References

[1] Rajak DK, Pagar DP, Menezes PL, Linul E. Fiber-Reinforced Polymer Composites: Manufacturing, Properties, and Applications. Polymers. 2019;11(10):1667. https://doi.org/10.3390/polym11101667

[2] Mortas N, Er O, Reis PNB, Ferreira JAM. Effect of corrosive solutions on composites laminates subjected to low velocity impact loading. Composite Structures. 2014;108:205-211. https://doi.org/10.1016/j.compstruct.2013.09.032

[3] Deng X, Zhang Z. Effects of Seawater Environment on the Degradation of GFRP Composites by Molecular Dynamics Method. Polymers. 2022;14(14):2804. https://doi.org/10.3390/polym14142804
[4] Gülsoy, M., Taşdemır, M., & Ö., H. Mechanical Properties of Polymers Filled with Iron Powder. International Journal of Polymeric Materials and Polymeric Biomaterials. 2008;57(3):258-265. https://doi.org/10.1080/00914030701473656
[5] Gungor, A. Mechanical properties of iron powder filled high-density polyethylene composites. Materials & Design. 2007;28(3):1027-1030. https://doi.org/10.1016/j.matdes.2005.11.003
[6] Basavarajappa S, Arun KV, Davim J. Effect of Filler Materials on Dry Sliding Wear Behavior of Polymer Matrix Composites - A Taguchi Approach. Journal of Minerals & Materials Characterization & Engineering. 2009;8(5):379-391. https://doi.org/10.4236/jmmce.2009.85034
[7] Salih SI, Nayyef S, Abd Alsalam AH, Hasan AM. Evaluation Mechanical Properties of Polymer Composites. Eng. & Tech. Journal. 2015;33(7):1348-1360. https://doi.org/10.30684/etj.2015.116706
[8] Ghorbanzadeh Ahangari M, Fereidoon A, Jahanshahi M, Sharifi N. Effect of nanoparticles on the micromechanical and surface properties of poly(urea-formaldehyde) composite microcapsules. Composites Part B: Engineering. 2014;56:450-455. https://doi.org/10.1016/j.compositesb.2013.08.071
[9] Vincent B, Natesan S, Anand G. Investigation on Thermo-Mechanical Behaviour of E Glass Fibre and Iron Oxide Filler Particles Reinforced Epoxy Composite. International Journal for Research in Applied Science and Engineering Technology. 2020;8:1522-1526. https://doi.org/10.22214/ijraset.2020.4245
[10] Megahed M, Fathy A, Morsy D, Shehata F. Mechanical Performance of glass/epoxy composites enhanced by micro- and nanosized aluminum particles. Journal of Industrial Textiles. 2019;51(1). https://doi.org/10.1177/1528083719874479
[11] Aravinth B, Vivek G, Gokulakrishanan S, Manikandan D. Synthesis and Mechanical Analysis of on iron powder of mixed glass fiber reinforced polymer composite Material. International Research Journal on Advanced Science Hub. 2020;2(11):26-29. https://doi.org/10.47392/irjash.2020.216
[12] Mao H, Abushammala H, Waste Iron Filings to Improve the Mechanical and Electrical Properties of Glass Fiber-Reinforced Epoxy (GFRE) Composites. Journal of Composites Science. 2023;7(3):90. https://doi.org/10.3390/jcs7030090
[13] Benmokrane B, Ali AH, Mohamed HM, ElSafty A, Manalo A. Laboratory assessment and durability performance of vinyl-ester, polyester, and epoxy glass-FRP bars for concrete structures. Composites Part B: Engineering. 2017;114:163-174. https://doi.org/10.1016/j.compositesb.2017.02.002
[14] Soles CL, Chang FT, Gidley DW, Yee AF. Contributions of the nanovoid structure to the kinetics of moisture transport in epoxy resins. Journal of Polymer Science Part B: Polymer Physics. 2000;38(5). https://doi.org/10.1002/(SICI)1099-0488(20000301)38:5<776::AID-POLB15>3.3.CO;2-1
[15] Mourad A-HI, Abdel-Magid BM, El-Maaddawy T, Grami ME. Effect of Seawater and Warm Environment on Glass/Epoxy and Glass/Polyurethane Composites. Applied Composite Materials. 2010;17(5):557-573. https://doi.org/10.1007/s10443-010-9143-1
[16] Silva MAG, da Fonseca BS, Biscaia H. On estimates of durability of FRP based on accelerated tests. Composite Structures. 2014;116:377-387. https://doi.org/10.1016/j.compstruct.2014.05.022
[17] Kaybal HB, Ulus H, Tatar AC, Demir O. Influence of seawater on mechanical properties of SiO2-epoxy polymer nanocomposites. Res. Eng. Struct. Mat. 2019;5(2):147-154. https://doi.org/10.17515/resm2018.61is0802

[18] Sukur EF, Kaybal HB, Ulus H, Avc A. Tribological behavior of epoxy nanocomposites under corrosive environment: effect of high-performance boron nitride nanoplatelet. Sigma Journal of Engineering and Natural Sciences. 2023;41(6). https://doi.org/10.14744/sigma.2022.00025
[19] Bian L, Xiao J, Zeng J, Xing S. Effects of seawater immersion on water absorption and mechanical properties of GFRP composites. Journal of Composite Materials. 2012;46(25):3151-3162. https://doi.org/10.1177/0021998312436992
[20] Abral H, Kadriadi D, Rodianus A, Mastariyanto P, Ilhamdi, Arief S, et al. Mechanical properties of water hyacinth fibers - polyester composites before and after immersion in water. Materials & Design. 2014;58:125-129. https://doi.org/10.1016/j.matdes.2014.01.043
[21] Bagherpour S, Bagheri R, Saatchi A. Effects of concentrated HCl on the mechanical properties of storage-aged fiber glass polyester composite. Materials & Design. 2009;30(2):271-274. https://doi.org/10.1016/j.matdes.2008.04.078
[22] Amaro AM, Reis PNB, Neto MA, Louro C. Effects of alkaline and acid solutions on glass/epoxy composites. Polymer Degradation and Stability. 2013;98(4):853-862. https://doi.org/10.1016/j.polymdegradstab.2012.12.029
[23] Mortas N, Er O, Reis PNB, Ferreira JAM. Effect of corrosive solutions on composites laminates subjected to low velocity impact loading. Composite Structures. 2014;108:205-211. https://doi.org/10.1016/j.compstruct.2013.09.032
[24] Lahlali D, Naffakh M, Dumon M. Cure kinetics and modeling of an epoxy resin cross-linked in the presence of two different diamine hardeners. Polymer Engineering & Science. 2005;45(12):1581-1589. https://doi.org/10.1002/pen.20274
[25] George GA, Cash GA, Rintoul L. Cure monitoring of aerospace epoxy resins and prepregs by Fourier transform infrared emission spectroscopy. Polymer International. 1996;41(2):169-182. https://doi.org/10.1002/(SICI)1097-0126(199610)41:2<169::AID-PI606>3.0.CO;2-2
[26] Voleník K, Lettner J, Hanousek F, et al. Oxides in plasma-sprayed chromium steel. Journal of Thermal Spray Technology. 1997;6:327-334. https://doi.org/10.1007/s11666-997-0067-8